Bioorganic & Medicinal Chemistry 16 (2008) 8706–8712

Contents lists available at ScienceDirect

Bioorganic & Medicinal Chemistry

journal homepage: www.elsevier.com/locate/bmc

Improvement of water solubility of non-competitive AMPA receptor antagonists by complexation with β-cyclodextrin

Rosanna Stancanelli [a,*], Vincenza Crupi [b], Laura De Luca [a], Paola Ficarra [a], Rita Ficarra [a], Rosaria Gitto [a], Marta Guardo [a], Nunzio Iraci [a], Domenico Majolino [b], Silvana Tommasini [a], Valentina Venuti [b]

[a] Dipartimento Farmaco-Chimico, Università di Messina, Viale Annunziata, 98168 Messina, Italy
[b] Dipartimento di Fisica, Università di Messina, C.da Papardo, S.ta Sperone 31, PO Box 55, 98166 S. Agata, Messina, Italy

ARTICLE INFO

Article history:
Received 10 June 2008
Revised 21 July 2008
Accepted 29 July 2008
Available online 5 August 2008

Keywords:
Tetrahydroisoquinoline derivatives
β-Cyclodextrin
UV–vis spectroscopy
FTIR-ATR spectroscopy
Molecular modelling

ABSTRACT

The (*R*,*S*)-2-acetyl-1-(4′-chlorophenyl)-6,7-dimethoxy-1,2,3,4-tetrahydroisoquinoline ((*R*,*S*)-**1**) was previously identified as a potent non-competitive AMPA receptor antagonist able to prevent epileptic seizures and reduce AMPA-induced current in electrophysiological experiments. Through the enantiomeric resolution of racemate by chiral HPLC we already demonstrated that the (*R*)-**1** enantiomer was the eutomer. Considering the poor water solubility, these compounds have been complexed with β-cyclodextrin (β-CyD).

The effect of β-cyclodextrin on the spectral features of molecules was quantitatively investigated, in fully aqueous medium by phase-solubility study and the obtained diagrams suggested that it forms complexes with a molar ratio 1:1. The binding constant ($K_{(R)\text{-}\mathbf{1}}$ = 15889 M^{-1}, $K_{(R,S)\text{-}\mathbf{1}}$ = 1079 M^{-1}) and the complexation efficiency (CE) were calculated. Then the solid complexes in 1:1 molar ratio were prepared by the co-precipitation method and the FTIR-ATR measurements were carried out in order to confirm the host–guest interactions that drive the complexation process, by monitoring the significant differences of the spectra of the complexes with respect to those of the corresponding physical mixtures in the same molar ratio. The experimental data have been compared with molecular modelling studies and we confirmed our hypothesis.

1. Introduction

The primary purpose of drug delivery systems is to transport the necessary amount of drug to the targeted site for a necessary period of time, both efficiently and precisely.[1–6] In this sense, the development of new strategies to drug delivery systems such as hydrogels, nano- and microspheres of biodegradable polymers, lyposomes and also host–guest systems, is an important research area, since some molecules used in pharmaceutical therapy cannot be delivered effectively through the conventional oral route. In this case, cyclodextrins (CyDs) have been considered useful drug delivery and carrier systems. CyDs are macrocyclic oligosaccharides obtained by an enzymatic transformation of starch. They are known in supramolecular chemistry as receptors able to include a range of organic, inorganic and biological molecules into their hydrophobic cavities via non-covalent interactions, such as hydrophobic and van der Waals interactions, hydrogen bonding, and release of ring strain in the CyD cavity.[7] In particular, the study of the host–guest interactions between CyDs and the enantiomers of a chiral molecule should provide a better insight into these interactions.

Glutamate (Glu), the major excitatory neurotransmitter in the vertebrate brain, plays an important role in neuronal activity operating through ionotropic (iGluRs) and metabotropic (mGluRs) receptors.[8] iGluRs are divided into *N*-methyl-D-aspartic acid (NMDA), 2-amino-3-(3-hydroxy-5-methylisoxazol-4-yl)propionic acid (AMPA) and kainate (KA) receptors.[9] It is well known that competitive and non-competitive antagonists of AMPA receptor (AMPAR) show to be promising in terms of their therapeutic potential for the prevention and treatment of a broad range of acute and chronic neurological disorders such as epilepsy, ischaemia and Parkinson's disease.[10,11]

In previous studies we identified new non-competitive AMPAR antagonists containing a isoquinoline skeleton.[12–21] Among this class of compounds, the (*R*,*S*)-2-acetyl-1-(4-chlorophenyl)-6,7-dimethoxy-1,2,3,4-tetrahydroisoquinoline ((*R*,*S*)-**1**, Fig. 1) demonstrated higher pharmacological effects when compared in *in vivo* and *in vitro* tests with other current AMPAR antagonists.[12,22] With the aim to go deep into the pharmacological profile, the enantiomeric resolution of compound (*R*,*S*)-**1** by chiral HPLC has been carried out. Then, we tested the activity of the two different

* Corresponding author. Tel.: +39 090 6766409; fax: +39 090 6766402.
E-mail address: rstancanelli@pharma.unime.it (R. Stancanelli).

0968-0896/$ - see front matter © 2008 Elsevier Ltd. All rights reserved.
doi:10.1016/j.bmc.2008.07.085

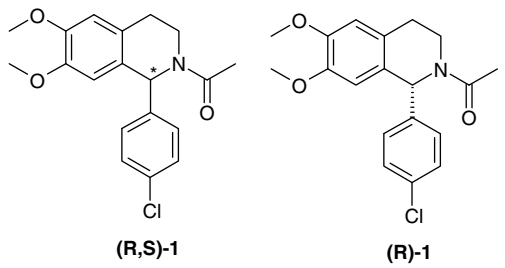

Figure 1. Chemical structure of (*R*,*S*)-2-acetyl-1-(4-chlorophenyl)-6,7-dimethoxy-1,2,3,4-tetrahydroisoquinoline (compound (*R*,*S*)-**1**).

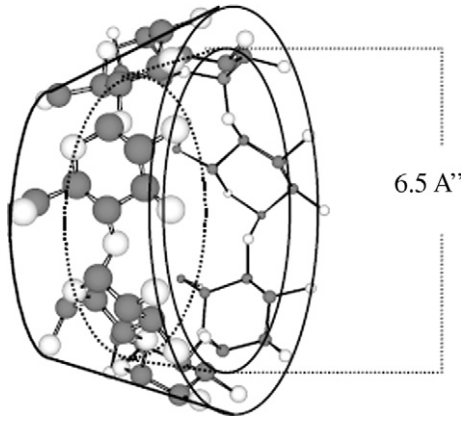

Figure 2. Spatial orientation of the different groups in β-cyclodextrin (β-CyD) molecule.

enantiomers and demonstrated that (*R*)-**1** enantiomer was more active than (*S*)-**1**, thus suggesting that chirality played an important role in the AMPAR recognition process as well as in the pharmacological effects.[20]

Compound (*R*,*S*)-**1** is very poorly soluble in water, and this is detrimental to its efficacy. The main goal of this work was to investigate the effect of β-cyclodextrin (β-CyD, Fig. 2) complexation on the UV absorption of the racemate and its enantiomers in pure water. In particular, the extent and mode of solubility enhancement exerted by β-CyD on these compounds have been experimentally measured under controlled conditions in aqueous solution, according to the method reported by Higuchi and Connors.[23] Then, the physical–chemical characterization of these complexes in solid state has been performed for a better understanding of non-covalent interactions present in these host–guest systems. The solid complexes of isoquinoline derivatives with the macrocycle in 1:1 molar ratio were obtained by the co-precipitation method. In addition, the corresponding physical mixtures in the same molar ratio have been prepared by simple blending and all the systems have been characterized by Fourier transform infrared (FTIR) absorption spectroscopy in attenuated total reflectance (ATR) geometry, evidencing significant changes in the vibrational spectra of the complexes with respect to physical mixtures and free molecules. This technique offers important advantages to the identification and characterization of pharmaceuticals with respect to the usual FTIR spectroscopy,[24–26] being non-invasive, since interferences due to the usual dispersion of sample in KBr or CsI pellets are avoided, requiring only micrograms of material and no sample manipulation.[27,28] It guarantees simple and fast in situ measurements, and high-quality and high-reproducible spectra that can in every respect be used quantitatively without any transformation. Its utility as an analytical method has been widely demonstrated.[29–31] Very recently, FTIR-ATR spectroscopy has also been proved to be a very promising choice for non-invasive real time monitoring of topical drug delivery,[32] and, in aqueous solutions, to be a potential alternative probe to investigate host–guest systems allowing also to determine the supramolecular complex stoichiometry.[33]

The obtained results have been complemented by a molecular modelling approach, as a tool for achieving detailed information on the geometry and the dynamical behaviour of the inclusion complexes.

2. Results and discussion

2.1. Phase-solubility studies

The solubility profiles for the complexes formation of (*R*)-**1** enantiomer and racemate with β-CyD are shown in Figure 3a and b, respectively.

It is evident that the apparent aqueous solubility of tetrahydroisoquinolines increase linearly as a function of macrocycle concentration suggesting the formation of 1:1 complexes. In particular, it was observed that the solubility in aqueous solution increases up to 5×10^{-3} M and 3×10^{-3} M for (*R*)-**1** enantiomer, and racemate,

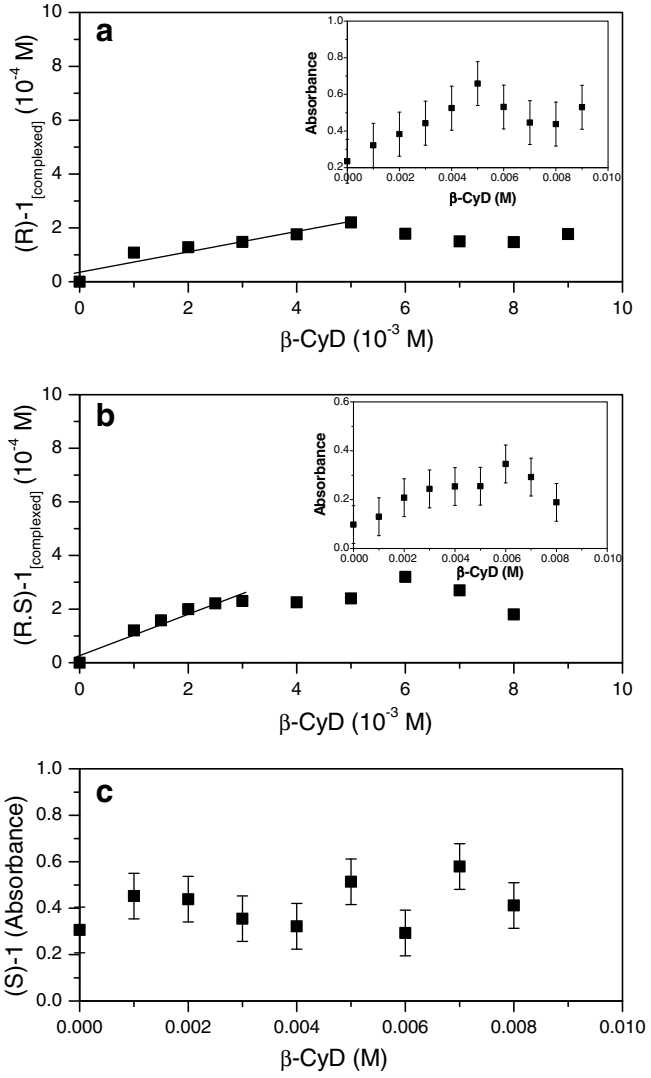

Figure 3. Concentration of complexed (*R*)-**1** (a), (*R*,*S*)-**1** (b) and (*S*)-**1** UV–vis phase-solubility diagram at different amounts of β-CyD in pure water at 25 °C. *Inset*: reports the phase-solubility diagram of (*R*)-**1** and (*R*,*S*)-**1** obtained by UV–vis spectra (path length *d* = 10 mm).

respectively; instead at higher concentrations of β-CyD we did not observe any further solubilisation since the studied molecules were totally complexed. The binding constant for a 1:1 complex is $K = [S{\cdot}CyD]/[CyD][S]$, where [S·CyD], [CyD] and [S] represent the equilibrium concentrations of the complexed substrate, free cyclodextrin and free substrate, respectively. This equation requires careful consideration when, as in the present case, the substrate is not fully soluble and amounts that exceed its solubility are used.

In this case the binding constants can be calculated by means of the phase-solubility technique, which allows the evaluation of the affinity between cyclodextrin and substrate.

In order to obtain [S·CyD] from the experimental quantities, it has to be considered that the concentration $C_S - S_0$ (being C_S the analytical concentration and S_0 the intrinsic water solubility of the drug, respectively) of the substrate not dissolved in water, acts as a reservoir for the formation of the complex when the cyclodextrin is added.

In the region where a linear increase was observed, a linear regression analysis was performed and the equations turned out to be as follows: $y = 0.0075x + 2E{-}05$ for (*R*,*S*)-**1**/β-CyD system; $y = 0.0375x + 4E{-}05$ for (*R*)-**1**/β-CyD system. The change of slope occurs when all the available compounds concentration $C_S{-}S_0$ are in the complexed form. From the slope of the linear fit the binding constant can be evaluated through $K = \alpha/(S_0(1-\alpha))$: $K_{(R)\text{-}\mathbf{1}} = 15889\ M^{-1}$ and $K_{(R,S)\text{-}\mathbf{1}} = 1079\ M^{-1}$. α is the slope of the linear plot reporting the amount of complexed (*R*)-**1** enantiomer and racemate as a function of β-CyD, and S_0 (10^{-6} M) is the intrinsic solubility of the drug in pure water experimentally obtained by distributing the guest molecule between water and organic solvent (*n*-hexane) after having already calculated the extinction molar coefficient (ε) of the molecule in *n*-hexane.[34]

A smaller K_C value indicates a too weak interaction, whereas a larger value indicates the possibility of limited release of drug from the complex thereby interfering with drug absorption.

The measured molar extinction coefficients of bound (*R*)-**1** enantiomer and racemate were determined as $\varepsilon_c = A_F - A_0/S_0$ (2985 and 1058 $mol^{-1}\ cm^{-1}$, respectively), A_F being the absorbance value of each molecule when complexed and A_0 the absorbance values of (*R*)-**1** enantiomer and racemate when $C_{CyD} = 0$.

For 1:1 drug/CyD complexes the complexation efficiency (CE) can be calculated from the slope of the phase-solubility diagram[35]: $CE = S_0{\cdot}K_{1:1} = [S{\cdot}CyD]/[CyD] = slope/(1 - slope)$ where [S·CyD] is the concentration of dissolved complex, [CyD] is the concentration of dissolved free cyclodextrin and slope is the slope of the phase-solubility profile. The CE for (*R*)-**1** and (*R*,*S*)-**1**/β-CyD complexes was 0.039 and 0.0075, respectively.

As far as the (*S*)-**1** enantiomer is concerned, it was not possible to observe the increase of solubility in water in presence of β-CyD (Fig. 3c) due to a different complexation mode as confirmed by molecular modelling study.

2.2. FTIR-ATR absorption measurements

Although the aforementioned results showed interactions between (*R*)-**1** enantiomer and racemate with β-CyD, suggesting the formation of real complexes by the co-precipitation method, FTIR-ATR spectroscopy was used in order to confirm this assumption. FTIR-ATR spectra were recorded to detect modifications, by a comparison between physical mixtures and inclusion complexes, in the spectral signals (band frequencies, widths and intensities) associated with specific structural groups of the drug molecules, so revealing the existence of intermolecular host–guest interactions.

The 3700 – 2600 cm^{-1} and 1750 – 700 cm^{-1} FTIR-ATR spectra of (*R*)-**1**, β-CyD, (*R*)-**1** + β-CyD physical mixture and (*R*)-**1**/β-CyD inclusion complex are compared in Figure 4. In the same way,

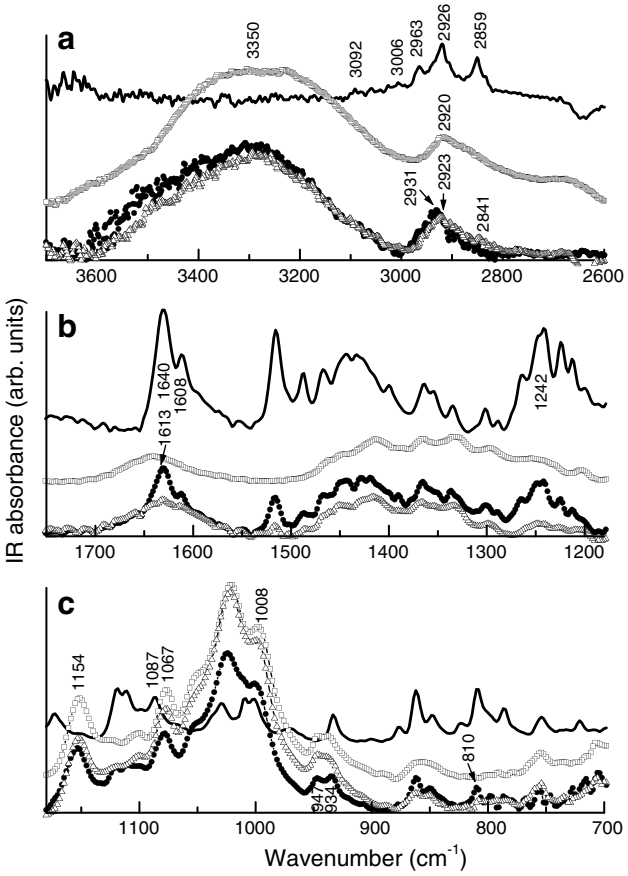

Figure 4. 3700–2600 cm^{-1} (a), 1750–1180 cm^{-1} (b) and 1180–700 cm^{-1} (c) FTIR-ATR spectra of (*R*)-**1** (solid line), β-CyD (open squares), (*R*)-**1** + β-CyD physical mixture (closed circles), and (*R*)-**1**/β-CyD inclusion complex (open triangles).

the 3700 – 2600 cm^{-1} and 1750 – 700 cm^{-1} FTIR-ATR spectra of (*R*,*S*)-**1**, β-CyD, (*R*,*S*)-**1** + β-CyD physical mixture and (*R*,*S*)-**1**/β-CyD inclusion complex are compared in Figure 5.

The FTIR-ATR spectra of (*R*)-**1** enantiomer and racemate show many vibrational bands. They are quite sharp, indicating that the molecules are in an almost structurally defined and regular environment (i.e., in a crystalline field). In particular, signals at ~3092–3006 2963, 2926 (connected to the C–H stretching vibration of the groups belonging to the ring) and 2859 cm^{-1} (C–H stretching vibration of the methyl groups), ~1640 cm^{-1} (C=O stretching) and ~1608 cm^{-1} (ring C=C stretching) are clearly revealed. Going on, the peaks in the 1520–1320 cm^{-1} region are due to the phenyl stretching vibration, probably convoluted with those associated to CH_3 bending vibrations of the alkyl groups, whereas the strong and complex band at 1320–950 cm^{-1} is connected to the CH rocking vibrations of the rings (~1242 cm^{-1}, multiple peak), convoluted with those associated to C–O– bonds (in the 1260–1000 cm^{-1} range) and C–N stretching (1180–900 cm^{-1}) and C–Cl aromatic stretching (~1087 cm^{-1}). Finally, the intense bands that appear in the 900–600 cm^{-1} region correspond to the out-of-plane bending of aromatic C–H bonds.

The FTIR-ATR spectrum of β-CyD has been already analysed in detail also by using second derivative computation and curve fitting.[24,36,37] As demonstrated, it shows prominent absorption bands at ~3350 cm^{-1} (O–H stretching vibrational modes of interstitial and intracavity water molecules together with those assigned to primary and secondary OH groups), ~2920 cm^{-1} (C–H stretching), ~1154 cm^{-1}, ~1067 cm^{-1} and ~1008 cm^{-1}, (C–H, C–O stretching vibrations).

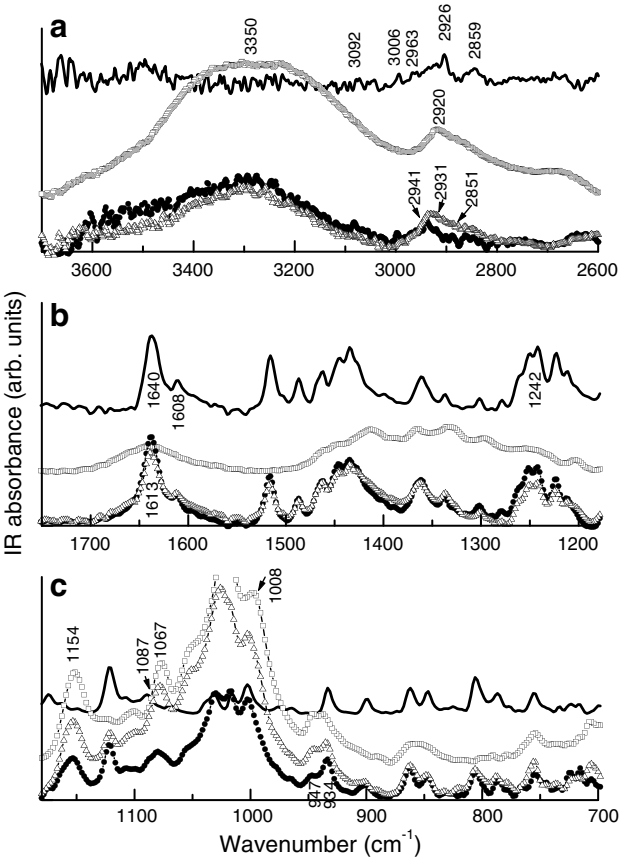

Figure 5. 3700–2600 cm^{-1} (a), 1750–1180 cm^{-1} (b) and 1180–700 cm^{-1} (c) FTIR-ATR spectra of (*R*,*S*)-**1** (solid line), β-CyD (open squares), (*R*,*S*)-**1** + β-CyD physical mixture (closed circles) and (*R*,*S*)-**1**/β-CyD inclusion complex (open triangles).

For both (*R*)-**1** enantiomer and racemate, the FTIR-ATR spectra of the physical mixtures can be considered as the result of a weighted addition of pure compound and β-CyD. This is a clear indication of the presence of two separate phases, crystalline compound and β-CyD, each of them maintained still intact.

On the contrary, differences (shifts, broadenings and/or attenuations) in the FTIR-ATR spectra of inclusion complexes with respect to those of physical mixtures are revealed, suggesting a modification of bonds strength and length of the drug environment, and appear much more pronounced if (*R*)-**1** enantiomer is used as guest molecule for complexation. In particular, by giving a look at the whole complexes spectra, we notice that they closely recall that of pure β-CyD. As already observed,[38] this fact confirms that inclusion complexes have been obtained: if the drug is included and not interposed between β-CyD molecules, its crystal structure will be completely rearranged and the system will assume a configuration similar to that of β-CyD.

As far as the high-frequency region is concerned, the spectra of the inclusion complexes showed modifications, with respect to the corresponding physical mixtures, of the O–H stretching bands corresponding to differently H-bonded OH groups. This result suggests that the existing hydrogen bonding environment involving the OH groups of β-CyD, interstitial and intracavity crystallization water molecules, may be disturbed because of the encapsulation of the drug. A diminishing in intensity of the high-frequency shoulder of the band is in particular revealed for both the analysed cases, together with a low-frequency shift ~14 cm^{-1} for (*R*)-**1**/β-CyD and ~7 cm^{-1} for (*R*,*S*)-**1**/β-CyD inclusion complexes, indicating that the observed changes in the involved H-bond scheme should imply an overall increasing of co-operativity involving longer lifetimes.

The C–H stretching signals revealed, respectively, at ~2931 cm^{-1} in (*R*)-**1** + β-CyD and ~2941 cm^{-1} in (*R*,*S*)-**1** + β-CyD physical mixtures, are low-shifted at ~2923 cm^{-1} and ~2931 cm^{-1} in the corresponding inclusion complexes. At the same time, the increasing of a low-frequency contribution, at ~2841 cm^{-1} in the (*R*)-**1**/β-CyD and ~2851 cm^{-1} in the (*R*,*S*)-**1**/β-CyD inclusion complex spectra is observed. These evidences let us to hypothesize an interaction, involving these functional groups, between guest and host as a consequence of encapsulation.

Going to lower frequencies, the changes revealed in the C=O stretching signal of the complexes, compared to physical mixtures, are very important in order to elucidate the molecular state of the drug upon complexation. Not so relevant modifications are observed in this region in the FTIR-ATR spectrum of (*R*,*S*)-**1**/β-CyD inclusion complex, whereas that of (*R*)-**1**/β-CyD inclusion complex indicated a definitely altered environment around the C=O bonds of the drug upon complexation, with the corresponding stretching band appearing reduced in intensity and much more enlarged. Both these evidences suggest an hindering of this vibration because of the restriction into the β-CyD cavity, definitely favoured in the case of (*R*)-**1** enantiomer. In particular, the intensity reduction can be attributable to the decrease of the dipole moment of the CO group due to hydrogen bond formation, between the CO groups of (*R*)-**1** enantiomer and the OH groups of β-CyD, or with the water molecules present in the cavity, as already observed for other inclusion complexes.[26] Again, the significant broadening of the band, that, as we will see, is revealed also for other vibrational peaks, could suggest an increase of the amorphous state, already revealed for different inclusion complexes,[39,40] that could be confirmed by X-ray diffractions measurements. The ring C=C stretching vibration peak of the drug, still evident at ~1613 cm^{-1} in the FTIR-ATR spectrum of the physical mixtures, is enlarged in the (*R*,*S*)-**1**/β-CyD inclusion complex spectrum, and definitely bumped in the case of (*R*)-**1**/β-CyD complex, suggesting the inclusion of this group inside the β-CyD cavity, that again appears more favourable for the (*R*)-**1** enantiomer. All the peaks associated to the phenyl stretching and CH_3 bending vibrations of the (*R*)-**1** enantiomer are strongly modified in their shape passing from physical mixture to inclusion complex. They show variations in the relative intensities, shifts in frequency and an overall bumping. From these observations, an inclusion of the aromatic ring of the (*R*)-**1** enantiomer inside the β-CyD cavity, involving the alkyl groups, can be hypothesized. This is also reinforced by the analysis of the CH rocking vibrations of the ring, that are almost unchanged in the physical mixture, whereas appear strongly modified in the inclusion complex. On the other side, small enlargements and relative intensity variations are detected in the case of (*R*,*S*)-**1**.

C-Clb stretching peak of pure drug appears completely overlapped by the more intense C–O signal of β-CyD in binary systems, becoming not more detectable. As far as the C–O and C–N stretching vibrations are concerned, the two peaks evident at ~947 and ~934 cm^{-1} in both the physical mixtures change in their relative intensities when passing to the inclusion complexes, an inversion is revealed in the case of (*R*)-**1**/β-CyD inclusion complex.

Finally, as main result for the changes revealed in the 900–600 cm^{-1} region, we notice, in the case of (*R*)-**1**/β-CyD inclusion complex, the disappearance, with respect to physical mixture, of the peak at ~810 cm^{-1}, indicative of the restrictions of the out-of-plane C–H bending vibration of the molecule, due to the cyclodextrin cavity.

These results indicate that, even with a similar basic complexation mechanism, β-CyD offers a more favourable accessibility to the (*R*)-**1** enantiomer with respect to the racemate, in agreement with our phase-solubility study.

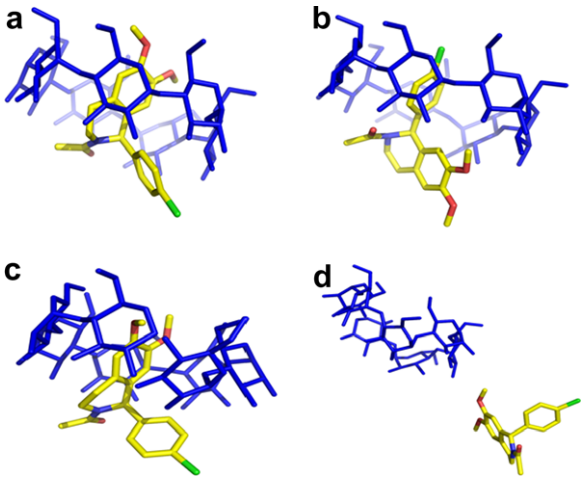

Figure 6. (*R*)-**1** and (*S*)-**1** complexed by β-CyD (blue): (a) and (b) represent the results of docking studies for (*R*)-**1** and (*S*)-**1**, respectively; (c) and (d) show the average structures from MD simulations for (*R*)-**1** and (*S*)-**1**, respectively.

2.3. Molecular modelling studies

In order to describe the main interactions between β-CyD and (*R*)-**1** enantiomer, as well as between β-CyD and (*S*)-**1** enantiomer, and to predict their stability, we carried out molecular modelling studies of the complexes.

This investigation concerns both docking studies and molecular dynamics (MD) simulations. The analysis of docking studies on (*R*)-**1**/β-CyD and (*S*)-**1**/β-CyD inclusion complexes revealed that the two different isomers are able to interact with β-CyD showing two different conceivable binding modes characterized by two different orientations (Fig. 6).

It is possible to observe from Figure 6(a) that in the case of (*R*)-**1** enantiomer the 1,2,3,4-tetrahydroisoquinoline frame was almost completely inserted on the interior of the β-CyD.

On the contrary, as reported in Figure 6(b), the (*S*)-**1** isomer assumed a different complexation mode and in particular the 1-4′-chlorophenyl substituent was in contact with β-CyD, while the 1,2,3,4-tetrahydroisoquinoline scaffold was found outside.

In order to gain further insight into binding modes and observe changes during time, we performed MD simulations on the inclusion complexes of β-CyD with the two different enantiomers. The data retrieved from simulations demonstrated a very different behaviour for the two host–guest complexes (Fig. 6(c) and (d)). In fact, the (*R*)-**1** enantiomer appeared to be constrained during the entire simulation process (see average structure in Fig. 6(c)), whereas, as shown in Figure 6(d), (*S*)-**1** enantiomer shifted rapidly away from cyclodextrin system.

The obtained results are in agreement with the experimental data obtained by phase-solubility and FTIR-ATR studies. In particular, this study furnishes a plausible explanation of the poor affinity between β-CyD and (*S*)-**1** enantiomer (see Section 2.1)

3. Conclusions

β-CyD has been used to improve the solubility of (*R*,*S*)-2-acetyl-1-(4′-chlorophenyl)-6,7-dimethoxy-1,2,3,4-tetrahydroisoquinoline ((*R*,*S*)-**1**) and (*R*)-**1** and (*S*)-**1** enantiomers in aqueous solution.

From phase-solubility data interactions between (*R*,*S*)-**1** and β-CyD, and between (*R*)-**1** and β-CyD have been revealed, giving rise, in both cases, to 1:1 inclusion complex, with apparent stability constants $K_C = 15889\ M^{-1}$ for (*R*)-**1**/β-CyD and $K_C = 1079\ M^{-1}$ for (*R*,*S*)-**1**/β-CyD complex, respectively. No complexation has been observed for (*S*)-**1** enantiomer.

The (*R*,S)-**1**/β-CyD and (*R*)-**1**/β-CyD complex formation has been confirmed, in solid phase, by FTIR-ATR spectroscopy, that allowed the investigation of the host–guest interactions driving the complexation process by the considerable differences revealed in the spectra of the physical mixtures with respect to those of the complexes. We demonstreted that the formation and/or modification of polar bonds play the main role in the inclusion phenomena. Even if a similar basic complexation mechanism is deduced for both racemate and (*R*)-**1** enantiomer, the encapsulation capability of β-CyD is showed to be enanched for this latter, in agreement with phase-solubility studies.

The obtained results were corroborated by molecular modelling calculations. (*R*)-**1** enantiomer turned out almost completely inserted in the β-CyD cavity during the entire simulation process, whereas only the 1-4′-chlorophenyl substituent of (*S*)-**1** isomer resulted in contact with the β-CyD cavity.

4. Experimental

4.1. Chemicals

The tetrahydroisoquinoline derivatives (*R*,S)-**1**, (*R*)-**1** and (*S*)-**1** were obtained following procedures reported in our previous paper.[20] β-Cyclodextrin (β-CyD, FW ≈ 1135.0, mp ≈ 290–300 °C dec) was purchased from Fluka Chemie (Switzerland).

4.2. UV–vis absorption measurements

Spectrophotometric measurements were carried out with a Perkin-Elmer UV–vis double beam spectrophotometer mod. Lambda 45 (Norwalk, USA), attached to a PC computer with proper software for total control of the experiments and data acquisition. One-centimetre rectangular quartz cells (Hellma) were employed in the 220–400 nm spectral range (scan speed 60 nm/min; slit = 2). For each measurement, the baseline was established by placing an aqueous solution of each cyclodextrin in the reference compartment at the same concentration of the sample. All measurements were carried out at 25.0 ± 0.01 °C. UV–vis spectroscopy was employed in the study of each molecule alone (10^{-4} M) and in the presence of increasing amounts of macrocycle ($1.0–9.0 \times 10^{-3}$ M) and the wavelength/nm max was 284.

4.3. Phase-solubility measurements

An excess of drugs was added to 10 ml of water or CyD aqueous solutions (0.00–0.009 M) in 10 ml stoppered conical flasks and shaken at constant temperature (25 °C) with a Telesystem stirring bath thermostat 15.40 with Telemodul 40C control unit. Flasks were sealed to avoid changes due to evaporation and magnetically stirred in a thermostated bath at 25.0 ± 0.01 °C. In order to avoid photodecomposition, all solutions containing the compounds were thoroughly protected from light. At equilibrium (72 h) aliquots were withdrawn, filtered (0.45 μm pore size, Sartorius Minisart®-SRP 15 PTFE) and spectrophotometrically assayed. Each experiment was carried out in triplicate. The apparent 1:1 stability constants of the (*R*,*S*)-**1**/β-CyD and (*R*)-**1**/β-CyD complexes were calculated from the phase-solubility diagrams. The phase-solubility profile is then constructed by assessing the effect of β-CyD on the apparent solubility of the drug. The practical and phenomenological implications of phase-solubility analysis were developed according to Higuchi and Connors method published in 1964 in their pioneering work[23] and reviewed by Connors.[41]

4.4. Preparation of solid inclusion complexes

(*R*,*S*)-**1**/β-CyD and (*R*)-**1**/β-CyD inclusion complexes with 1:1 molar ratio were prepared by co-precipitation method, by shaking the appropriate amounts of drug and macrocycle in water at 60 °C. Each mixture was stirred for 1 h, under controlled temperature (25.0 ± 0.01 °C). The reaction mixture was cooled in the refrigerator (4 °C) for about 24 h and the water was subsequently evaporated under vacuum (~30 °C), obtaining the solid complexes. Uncomplexed drug was filtered, through Sartorius Minisart®-SRP 15 PTFE 0.45 μm filters, prior to solution evaporation thus, obtaining the solid complex.

4.5. Preparation of physical mixtures

The 1:1 molar ratio (*R*,*S*)-**1** + β-CyD and (*R*)-**1** + β-CyD physical mixtures were prepared by mixing the single components in an agate mortar until the mixture was homogeneous.

4.6. FTIR-ATR absorption measurements

A Bomem DA8 Fourier transform infrared spectrometer, with a Globar source, a KBr beamsplitter and a thermoelectrically cooled deuterated triglycene sulfate (DTGS) detector was used. For all the investigated samples, the measurements were performed at room temperature (25 ± 0.01 °C). A Golden Gate diamond ATR system, just based on the attenuated total reflectance technique, contained the powders. The FTIR-ATR spectroscopy involves the collection of radiation reflected from the interface, between the sample (solid or liquid) and a prism (ATR crystal), in which the evanescent wave, penetrated from the prism into the sample, is absorbed by the substances and reflected to the detector. A property of the evanescent wave that makes ATR a powerful technique is that the intensity of the wave decays exponentially with a distance from the surface of the ATR crystal. The distance, on the order of micrometers, makes ATR generally insensitive to sample thickness, allowing the analysis of thick or strongly absorbing samples.

All spectra were recorded within a range of 4000–600 cm^{-1}. In order to get a good signal-to-noise ratio and high-reproducibility, each spectrum was collected with a resolution of 2 cm^{-1}, and is an average of 100 repetitive scans automatically added for each run. All the measurements were performed in a dry atmosphere. To check a possible unwanted effect induced by wetting and/or drying phenomena when the sample holder was filled with dry nitrogen, IR spectra in presence and absence of air were compared without showing any significant difference. All the spectra were normalized in order to take the effective number of absorbers into account.

No mathematical correction (e.g., smoothing) was done, and spectroscopic manipulation such as baseline adjustment and normalization were performed using the Spectracalc software package GRAMS (Galactic Industries, Salem, NH, USA).

4.7. Molecular modelling

4.7.1. Docking experiments

β-CyD and ligands structures were constructed using the 3D-Sketcher tool available in Maestro[42] and then submitted to 10,000 steps of Polak-Ribiere conjugate gradient energy minimization by means of the Macromodel software,[43] using OPLS-2005 as force-field,[44] and GB/SA model as solvation treatment.[45] Docking studies were performed with the Glide program[46] using the centroid of cyclodextrin to centre the enclosing box used as docking space.

Docking poses with RMS deviation <3 Å were discarded and at most 20 docking poses were retrieved.

The best scoring pose of each enantiomer was selected.

4.7.2. Molecular dynamics

Molecular dynamics (MD) simulations were performed in order to observe changes in time.

Each structure was surrounded by a sphere of explicit water molecules with a radius of 25 Å, and the spherical harmonic boundary conditions were applied.

The hydrate complexes underwent a preliminary minimization; at first a minimization of the solvent with cyclodextrin and ligand constrained and then a minimization of all. MD simulations were organized into an initial period of heating from 0 to 300 K over 3000 iterations (3 ps) followed by 300 ps of equilibration phase with constant temperature.

The final coordinates and velocities of this stage were used to initiate a simulation of 5 ns.

The simulation was carried out using NAMD2.51[47] implemented on a 1.3 GHz Intel Itanium 2 CPU (see Acknowledgments).

The atom types were assigned using force-field CHARMM v22 and the atomic charges according the Gasteiger–Marsili method. The trajectory obtained was analysed using VEGA.[48]

Acknowledgments

We gratefully acknowledge expert technical assistance at C.E.C.U.M. Scientific Computing Service of University of Messina by Dora Magaudda (coordinator), Filippo Sciacca and Francesco Lo Re. This work was supported by University of Messina and MiUR.

References and notes

1. Sudhakar, Y.; Kuotsu, K.; Bandyopadhyay, A. K. *J. Control. Release* **2006**, *114*, 15–40.
2. George, M.; Abraham, T. E. *J. Control. Release* **2006**, *114*, 1–14.
3. Couvreur, P.; Gref, R.; Andrieux, K.; Malvy, C. *Prog. Solid State Chem.* **2006**, *34*, 231–235.
4. Sajeesh, S.; Sharma, C. P. *Int. J. Pharm.* **2006**, *325*, 147–154.
5. Rajendrakumar, K.; Madhusudan, S.; Pralhad, T. *Eur. J. Pharm. Biopharm.* **2005**, *60*, 39–46.
6. Shen, Y.; Yang, S.; Wu, L.; Ma, X. *Spectrochim. Acta A* **2005**, *61*, 1025–1028.
7. Huang, M. J.; Watts, J. D.; Bodor, N. *Int. J. Quant. Chem.* **1997**, *64*, 711–719.
8. Kew, J. N.; Kemp, J. A. *Psychopharmacology* **2005**, *179*, 4–29.
9. Wollmuth, L. P.; Sobolevsky, A. I. *Trends Neurosci.* **2004**, *27*, 321–328.
10. Gitto, R.; Barreca, M. L.; De Luca, L.; Chimirri, A. *Exp. Opin. Ther. Patents* **2004**, *14*, 1199–1213.
11. Catarzi, D.; Colotta, V.; Varano, F. *Med. Res. Rev.* **2007**, *27*, 239–278.
12. Gitto, R.; Barreca, M. L.; De Luca, L.; De Sarro, G.; Ferreri, G.; Quartarone, S.; Russo, E.; Constanti, A.; Chimirri, A. *J. Med. Chem.* **2003**, *46*, 197–200.
13. Barreca, M. L.; Gitto, R.; Quartarone, S.; De Luca, L.; De Sarro, G.; Chimirri, A. *J. Chem. Inf. Comput. Sci.* **2003**, *43*, 651–655.
14. Chimirri, A.; De Sarro, G.; Quartarone, S.; Barreca, M. L.; Caruso, R.; De Luca, L.; Gitto, R. *Pure Appl. Chem.* **2004**, *76*, 931–939.
15. De Sarro, G.; Russo, E.; Ferreri, G.; Gallelli, L.; Gitto, R.; Barreca, M. L.; Chimirri, A. *Naunyn-Schmiedebergs Arch. Pharmacol.* **2004**, *369*, R167.
16. Gitto, R.; Barreca, M. L.; Francica, E.; Caruso, R.; De Luca, L.; Russo, E.; De Sarro, G.; Chimirri, A. *Arkivoc* **2004**, 170–180.
17. Arstad, E.; Gitto, R.; Chimirri, A.; Caruso, R.; Constanti, A.; Turton, D.; Hume, S. P.; Ahmad, R.; Pilowsky, L. S.; Luthra, S. K. *Bioorg. Med. Chem.* **2006**, *14*, 4712–4717.
18. De Luca, L.; Gitto, R.; Barreca, M. L.; Caruso, R.; Quartarone, S.; Citraro, R.; De Sarro, G.; Chimirri, A. *Arch. Pharm. (Weinheim)* **2006**, *339*, 388–400.
19. Gitto, R.; Caruso, R.; Pagano, B.; De Luca, L.; Citraro, R.; Russo, E.; De Sarro, G.; Chimirri, A. *J. Med. Chem.* **2006**, *49*, 5618–5622.
20. Gitto, R.; Ficarra, R.; Stancanelli, R.; Guardo, M.; De Luca, L.; Barreca, M. L.; Pagano, B.; Rotondo, A.; Bruno, G.; Russo, E.; De Sarro, G.; Chimirri, A. *Bioorg. Med. Chem.* **2007**, *15*, 5417–5423.
21. Gitto, R.; Pagano, B.; Citraro, R.; Scicchitano, F.; De Sarro, G.; Chimirri, A. *Eur. J. Med. Chem.*, in press. doi:10.1016/j.ejmech.2008.02.025.
22. Rizzo, M.; Ventrice, D.; Casale, F.; De Sarro, G.; Gitto, R.; Chimirri, A. *J. Chromat. B Anal. Technol. Biomed. Life Sci.* **2007**, *850*, 161–167.
23. Higuchi, T.; Connors, K. A. *Adv. Anal. Chem. Instr.* **1965**, *4*, 117–212.
24. Crupi, V.; Ficarra, R.; Guardo, M.; Majolino, D.; Stancanelli, R.; Venuti, V. *J. Pharm. Biomed. Anal.* **2007**, *44*, 110–117.

25. Stancanelli, R.; Ficarra, R.; Cannavà, C.; Guardo, M.; Calabrò, M. L.; Ficarra, P.; Ottanà, R.; Maccari, R.; Crupi, V.; Majolino, D.; Venuti, V. *J. Pharm. Biomed. Anal.* **2008**, *47*, 704–708.
26. Cannavà, C.; Crupi, V.; Ficarra, P.; Guardo, M.; Majolino, D.; Stancanelli, R.; Venuti V. *Vib. Spectrosc.*, in press. doi:10.1016/j.vibspec.2007.12.013.
27. Crupi, V.; Longo, F.; Majolino, D.; Venuti, V. *J. Chem. Phys.* **2005**, *123*, 154702.
28. Hahn, B. D.; Neubert, R. H. N.; Wartewig, S.; Christ, A.; Hentzsch, C. *J. Pharm. Sci.* **2000**, *89*, 1106–1113.
29. Armenta, S.; Garrigues, G.; de la Guardia, M.; Rondeau, P. *Anal. Chim. Acta* **2005**, *289*, 99–106.
30. Carolei, L.; Gutz, I. G. R. *Talanta* **2005**, *66*, 118–124.
31. Ilario, R.; Iñón, F. A.; Garrigues, S.; de la guardia, M. *Talanta* **2006**, *69*, 469–480.
32. Wartewig, S.; Neubert, R. H. H. *Adv. Drug Del. Rev.* **2005**, *57*, 1144–1170.
33. de Sousa, F. B.; Oliveira, M. F.; Lula, I. S.; Sansiviero, M. T. C.; Cortés, M. E.; Sinisterra, R. D. *Vib. Spectrosc.* **2008**, *46*, 57–62.
34. Stancanelli, R.; Mazzaglia, A.; Tommasini, S.; Calabrò, M. L.; Villari, V.; Guardo, M.; Ficarra, P.; Ficarra, R. *J. Pharm. Biomed. Anal.* **2007**, *44*, 980–984.
35. Loftsson, T.; Hreinsdóttir, D.; Másson, M. Evaluation of cyclodextrin solubilization of drugs. *Int. J. Pharm.* **2005**, *302*, 18–28.
36. Gavira, J. M.; Hernanz, A.; Bratu, I. *Vib. Spectrosc.* **2003**, *32*, 137–146.
37. Bratu, I.; Veiga, F.; Fernandes, C.; Hernanz, A.; Gavira, J. M. *Spectroscopy* **2004**, *18*, 459–467.
38. Montassier, P.; Duchêne, D.; Poelmann, M. C. *Int. J. Pharm.* **1997**, *153*, 199–209.
39. Bratu, I.; Hernanz, A.; Gavira, J. M.; Bora, G. H. *Rom. J. Phys.* **2005**, *50*, 1063–1069.
40. Mura, P.; Bettinetti, G. P.; Manderioli, A.; Faucci, M. T.; Bramanti, G.; Sorrenti, M. *Int. J. Pharm.* **1998**, *166*, 189.
41. Connors, K. A.. In *Cyclodextrins Comprehensive Supramolecular Chemistry*; Szejtli, J., Osa, T., Eds.; Pergamon: Oxford, UK, 1996; Vol. 3, pp 205–241.
42. Maestro; version 8.0; Schrödinger LLC: New York, 2007.
43. Macromodel; version 9.5; Schrödinger LLC: New York, 2007.
44. Jorgensen, W. L.; Maxwell, D. S.; Tirado-Rives, J. *J. Am. Chem. Soc.* **1996**, *118*, 11225–11236.
45. Clark Still, W.; Tempczyk, A.; Hawley, R. C.; Hendrickson, T. *J. Am. Chem. Soc.* **1990**, *112*, 6127–6129.
46. Friesner, R. A.; Banks, J. L.; Murphy, R. B.; Halgren, T. A.; Klicic, J. J.; Mainz, D. T.; Repasky, M. P.; Knoll, E. H.; Shaw, D. E.; Shelley, M.; Perry, J. K.; Sander, L. C.; Shenkin, P. S. *J. Med. Chem.* **2004**, *47*, 1739–1749.
47. Kalè, L. S.; Bhandarkar, R.; Brunner, M.; Gursoy, R.; Krawetz, A.; Phillips, N.; Shinozaki, J.; Varadarajan, A.; Schulten, K. *J. Comput. Phys.* **1999**, *151*, 283–312.
48. Pedretti, A.; Villa, L.; Vistoli, G. *J. Mol. Graph. Model.* **2002**, *21*, 47–49.